

Durable Response to Nivolumab in a Patient With Hepatic Sarcomatoid Carcinoma: Evolutive Characterization of Genomic and Immunohistochemical PD-L1 Expression Findings

Marcello M. Queiroz, MD¹; Rodrigo R. Munhoz, MD¹; Cibele Masotti, PhD²; Larissa M. Souza, MSc²; Luiz G.C.A. Lima, MD³; Paula F. Asprino, PhD²; Maria Dirlei F.S. Begnami, MD, PhD³; Anamaria A. Camargo, PhD²; and Fabiana Bettoni, PhD²

JCO Precis Oncol 6:e2200163. © 2022 by American Society of Clinical Oncology

Creative Commons Attribution Non-Commercial No Derivatives 4.0 License 

Introduction

Sarcomatoid carcinomas are malignant neoplasms characterized by a heterologous composition of both epithelial/carcinomatous and spindle cell/sarcomatous features.^{1,2} These neoplasms may arise from various primary sites, and the frequently reported presentations include uterine, pulmonary, and genitourinary sarcomatoid carcinomas. Currently, little is known about the etiology and pathogenesis of these tumors. Primary hepatic sarcomatoid carcinomas (HSCs) are rare entities that are identified in approximately 2% of surgically resected hepatic tumors and are marked by an ominous prognosis and a high risk of recurrence and metastases.^{1,3} The histogenesis of HSC is related to dedifferentiation of the originating epithelioid component. Its imaging features are nonspecific, and pathological findings frequently display overlapping characteristics. This makes the distinction of HSC from hepatocellular carcinomas, intrahepatic cholangiocarcinomas, and soft tissue sarcomas challenging.⁴ Owing to their heterogeneous nature, biopsies are often misleading and may result in incorrect interpretations.

Surgical resection is the treatment of choice for patients with localized disease.⁵ Nevertheless, venous invasion, local recurrence, intrahepatic dissemination, and distant metastases are frequent, and this leads to a dismal prognosis such that approximately 50% of patients die during the first year after surgery.³ The optimal treatment remains unclear for those with advanced disease, and alternatives are often extrapolated from those applied to purely epithelioid-related entities.

Given the rarity of these tumors, there are limited data about the molecular alterations and potentially actionable targets. Recently, Zhang et al⁶ performed a comprehensive mutational analysis of 15 HSC tumor samples and reported a high mutation rate in genes involved in cell cycle regulation. Pertinently, mutations in *CDKN2A*

were detected in 26.6% of HSC cases and were associated with reduced progression-free and overall survival.

This case report describes a patient diagnosed with metastatic HSC enriched with potential biomarkers of sensitivity to immunotherapy. The patient was treated with nivolumab, which resulted in a durable response. In addition to characterizing the evolution of programmed death-ligand 1 (PD-L1) expression, sequential molecular analyses of samples obtained from different disease sites were performed to identify the molecular alterations that could drive tumorigenesis and secondary resistance to treatment.

Materials and Methods

See the Data Supplement (online).

Ethics

This study was approved by the Hospital Sirio-Libanês Research Ethics Board (HSL2018-59), and the patient provided written informed consent for study participation and the collection and publication of clinical and molecular data.

Case Report and Results

A 38-year-old woman who was otherwise healthy, presented for evaluation because of a lytic skull lesion associated with metastatic disease. Three years before admission, she reported the diagnosis of what was initially interpreted as a hepatic adenoma, identified during routine ultrasonography (US), and described as a hyperechogenic nodule in segments VI/VII that measured 8.5 × 6.6 cm. Two years after this episode, the patient's clinical course was complicated by hemorrhagic shock attributed to a hepatic hematoma in the corresponding hepatic segment, which was treated with selective hepatic embolization. Biopsies were not performed, and the patient was followed up with alternate US and computed tomography (CT) scans that showed a progressive reduction of the hematoma. More than 16 months after embolization, she sought medical attention because of persistent pain in the right parieto-occipital region. Head CT

ASSOCIATED CONTENT

Data Supplement

Author affiliations and support information (if applicable) appear at the end of this article.

Accepted on July 19, 2022 and published at ascopubs.org/journal/po on August 31, 2022; DOI <https://doi.org/10.1200/P0.22.00163>

revealed a 1.8-cm lytic lesion in the right parietal bone, which was resected (sample 1—baseline bone lesion). Pathology analyses showed a poorly differentiated malignancy with mesenchymal features and epithelioid components that were marked by high cellularity and frequent atypia and extensive necrosis, with a mitotic count of 26 mitoses/10 high-power fields. Immunohistochemical stainings were positive for vimentin and cytokeratins AE1-AE3 and negative for CD34, ERG, desmin, S100, HMB-45, CK7, CK20, and TTF-1, which was consistent with the diagnosis of a sarcomatoid carcinoma. This was confirmed through a subsequent pathology revision.

Initial staging was completed by an ^{18}F -labeled fluorodeoxyglucose positron emission tomography CT (18F-FDG PET-CT) scan that revealed increased FDG uptake in a dominant hepatic mass that measured 9.1×6.1 cm in segments VI/VII, suggestive of the primary site, in at least four pulmonary nodules measuring up to 1.8 cm and in a lytic lesion in the metadiaphyseal region of the right femur that measured approximately 3.3 cm.

Following multidisciplinary discussions and on the basis of the diagnosis of HSC with pulmonary and bone metastases, the decision was made to proceed with first-line liposomal doxorubicin at a dose of 50 mg/m^2 administered intravenously once every 28 days and stereotactic body radiation therapy to the femoral lesion.

Concurrent with systemic frontline chemotherapy, additional analyses included a next-generation sequencing–based comprehensive genome profiling test of the previously resected bone metastasis (sample 1) through a commercially available platform. Next-generation sequencing revealed *CD274* (*PD-L1*) and *PDCD1LG2* (*PD-L2*) amplifications, *CDKN2A/B* loss, deletion of exons 2-7 of the *CTNNB1* gene, and *KRAS* A146T, *PIK3CA* E542K, and *FANCC* A349fs*25 somatic mutations. A tumor mutational burden of 7 mutations/Mb was also reported. Notably, immunohistochemistry for PD-L1 expression using the SP263 antibody clone showed 100% positivity in tumor cells.

Restaging scans after two cycles of liposomal doxorubicin were consistent with progressive disease

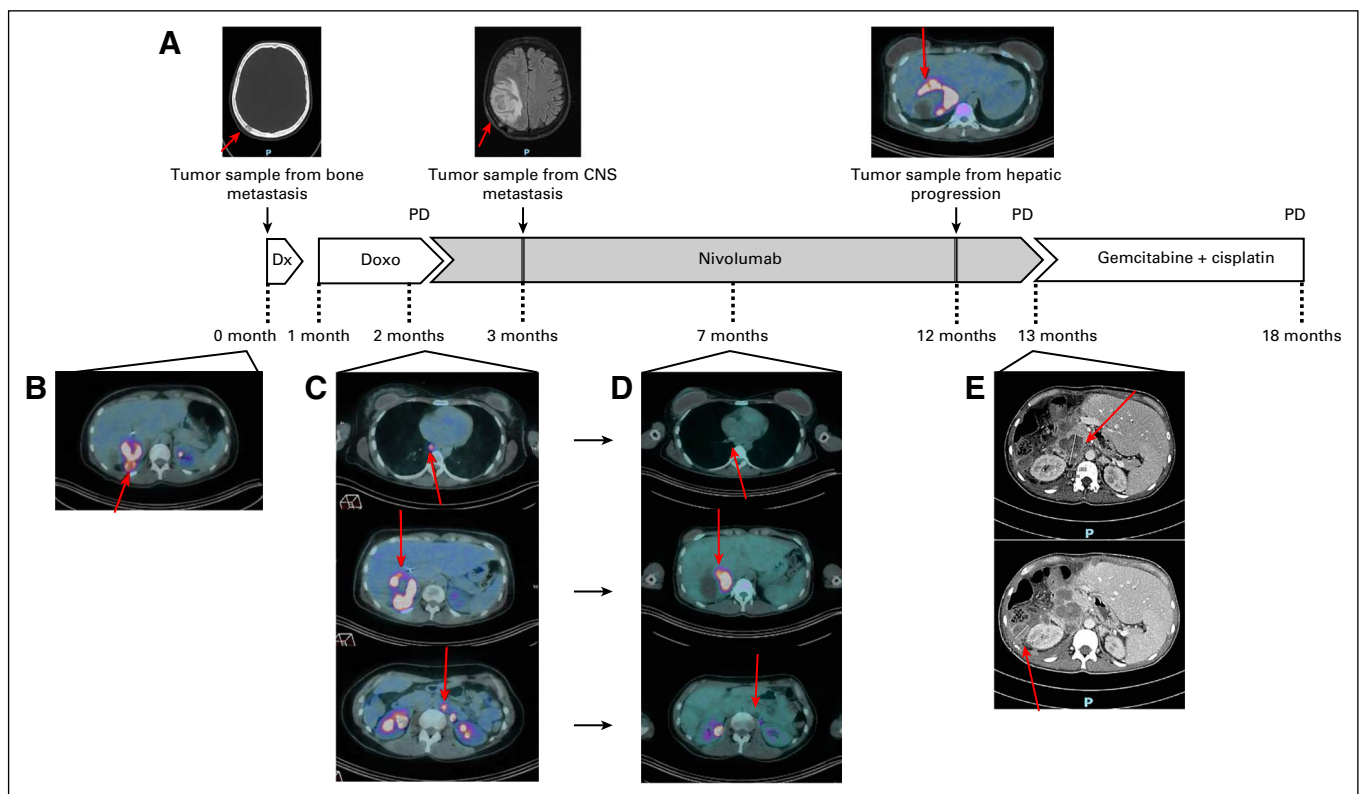


FIG 1. Treatment timeline from the beginning of metastatic disease. (A) Tumor imaging from baseline bone lesion (sample 1), central nervous system oligoprogression after exposure to nivolumab (sample 2), and hepatic progression after exposure to nivolumab (sample 3). (B) PET-CT image evidencing of the hepatic lesion at diagnosis, which was considered time zero of patient treatment. (C) PET-CT images at 2 months, before the initiation of nivolumab treatment. From top to bottom: images with the lung, liver, and para-aortic lymph nodes metastases. (D) Restaging PET-CT at 7 months after metastatic disease diagnosis, during nivolumab treatment. From top to bottom: images demonstrating response in the lung, liver, and para-aortic lymph node metastases. (E) MRI scan showing progression during nivolumab treatment with peritoneal nodules, approximately 13 months after the diagnosis of metastatic disease. Dx, diagnosis; Doxo, liposomal doxorubicin; MRI, magnetic resonance imaging; PET-CT, positron emission tomography-computed tomography; PD, progression of disease.

characterized by increased size and number of pulmonary nodules, increased hypermetabolic activity in the primary hepatic mass, and new nodal lesions. Because of the paucity of standard therapies in this scenario, and according to the results of the ancillary tests, the patient was treated with second-line nivolumab, administered intravenously at a dose of 3 mg/kg once every 14 days. Initial stabilization followed a reduction in size, and FDG uptake by the primary lesions was documented in subsequent PET-CT scans (Fig 1) along with resolution of the nodal pulmonary metastases. Nevertheless, interval magnetic resonance imaging prompted by recurrent headaches revealed a new contrast-enhancing brain lesion located in the corticosubcortical area of the right parietal region that measured 3.1 × 2.2 cm, 1 month after the initiation of nivolumab treatment. As this finding represented the only focus of progressive disease, the patient underwent metastasectomy (sample 2—CNS progression) followed by additional radiation therapy to the surgical bed and continued systemic treatment with nivolumab. After 23 cycles of nivolumab and almost 1 year of treatment associated with good tolerance and

continued disease control, a focal increase in size and hypermetabolic activity in the primary hepatic tumor were documented, without additional foci of active disease. At this point, a hepatic trisegmentectomy was recommended (sample 3—hepatic progression). The patient developed short-interval multifocal disease progression, with new nodal lesions and signs of peritoneal involvement. A salvage regimen with gemcitabine and cisplatin was attempted; treatment was unsuccessful at this point, and the patient died because of complications resulting from progressive disease.

Hematoxylin and eosin staining of the primary hepatic tumor confirmed the histopathologic diagnosis of sarcomatoid carcinoma (Fig 2A). Immunohistochemical analysis of the same specimen indicated negative immunostaining for Hep Par-1 (Fig 2B) and β -catenin (Fig 2C) and vimentin positivity in both sarcomatoid and carcinomatous components (Fig 2D). A similar immunohistochemistry pattern was observed in the metastatic tumor samples (data not shown).

We then evaluated PD-L1 expression over time, which showed a marked decrease in positivity in samples obtained from progressing lesions. Baseline bone metastasis (sample 1)

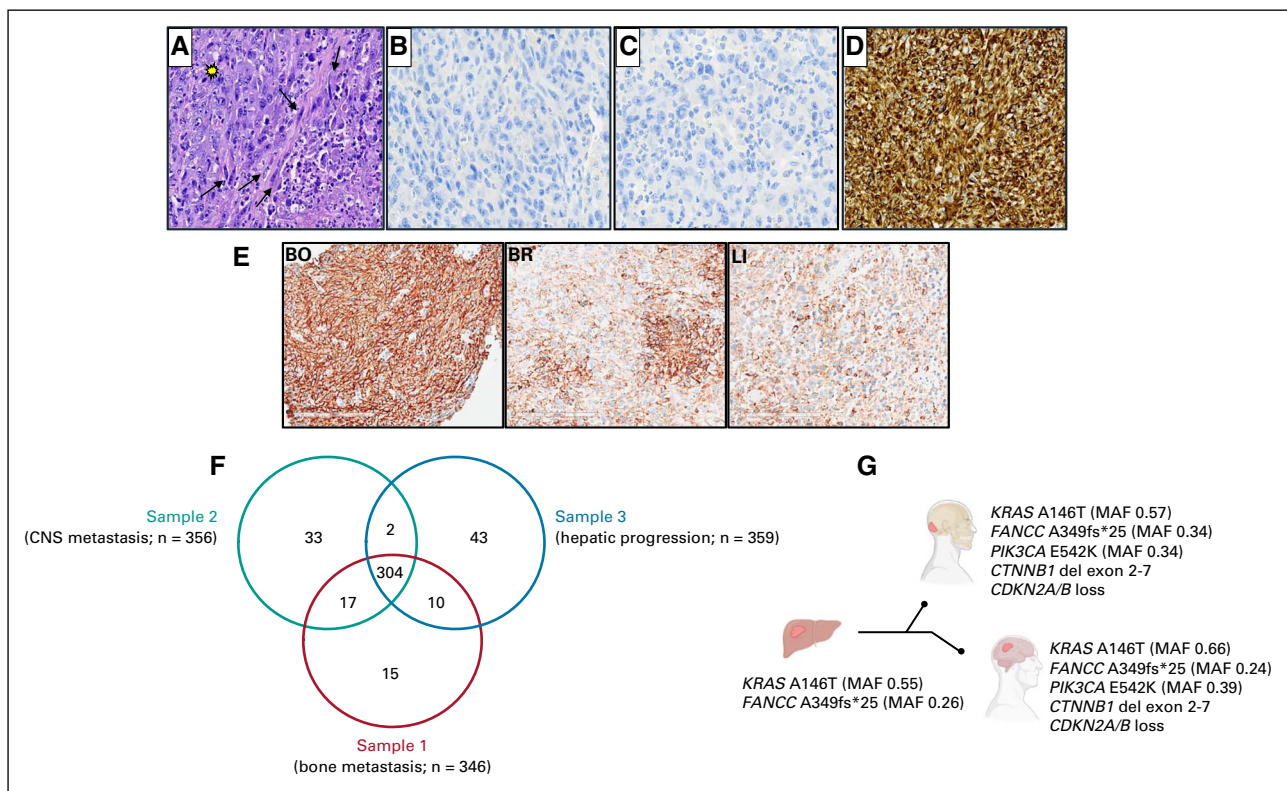


FIG 2. Serial analyses of tumor specimens through molecular characterization and IHC findings. (A) Hematoxylin and eosin staining indicating epithelioid cells (star) and pleomorphic, spindle cells (sarcomatous component—arrows; 40 \times). (B) Negative immunostaining with Hep Par-1 (40 \times). (C) Negative immunostaining of β -catenin (40 \times). (D) Vimentin positivity in both sarcomatoid and carcinomatous components (20 \times). (E) PD-L1 expression. (F) Venn diagram indicating common and exclusive mutations detected in each sample. (G) Temporal evolution of genetic variants identified in tumor samples. BO, sample 1—bone metastasis at baseline (pretreatment); BR, sample 2—central nervous system focal metastasis of progressive disease after initial response to nivolumab; IHC, immunohistochemistry; LI, sample 3—focus of subsequent hepatic progression; MAF, minor allele frequency; PD-L1, Programmed death-ligand 1. Credit: Figure 2G was created using BioRender.

showed expression of PD-L1 in 100% of tumor cells; analysis of brain metastasis (sample 2) showed that 40% of positive tumor cells are grouped in small clusters, whereas the focus of hepatic progression (sample 3) showed 20% positivity, with sparse positive tumor cells (Fig 2E).

To better characterize the temporal evolution and molecular aspects of this disease, serial analyses of the obtained specimens (sample 1—baseline bone lesion; sample 2—central nervous system oligoprogression after exposure to nivolumab; and sample 3—hepatic progression after exposure to nivolumab) were performed, including whole-exome sequencing and assessment of PD-L1 expression. The average sequencing coverage was 194× (sample 1—193×, sample 2—225×, and sample 3—164×), and an average of 354 somatic mutations (including nonsynonymous single nucleotide variants and indels) were detected per sample. Most of these mutations (n = 304) were common to all three lesions (Fig 2F). Mutations in *KRAS* and *FANCC* were identified as truncal mutations, whereas the *PIK3CA* mutation, deletion of exons 2-7 of the *CTNNB1* gene, and *CDKN2A/B* loss were identified solely in metastatic samples (Fig 2G). Notably, the loss of *CDKN2A/B* was also confirmed by ddPCR analysis. Amplifications of *CD274* (*PD-L1*) and

PDCD1LG2 (*PD-L2*) that were initially observed in sample 1 were not observed in samples 2 and 3. In addition, tumor mutational burden was estimated for each sample, and no significant difference was observed among the different lesions (sample 1—8.33 muts/Mb, sample 2—8.35 muts/Mb, and sample 3—8.22 muts/Mb).

Discussion

See the Data Supplement.

In conclusion, HSC remains an entity characterized by poor prognosis and limited treatment options, especially in metastatic cases. Our case report highlights the importance of molecular profiling in the era of personalized care, particularly in challenging scenarios with scarce evidence to guide treatment decisions. This case report adds to the limited available literature and suggests that immune checkpoint inhibitors treatment may represent an effective strategy for select patients with metastatic HSC, particularly for cases enriched with potential biomarkers of sensitivity to immunotherapy. Nevertheless, efforts are mandatory to better characterize and overcome the resistance mechanisms that often limit the efficacy of immune checkpoint inhibitors.

AFFILIATIONS

¹Oncology Center, Hospital Sírio-Libanês, São Paulo, SP, Brazil

²Molecular Oncology Center, Hospital Sírio-Libanês, São Paulo, SP, Brazil

³Department of Pathology, Hospital Sírio-Libanês, São Paulo, SP, Brazil

CORRESPONDING AUTHOR

Fabiana Bettoni, PhD, Molecular Oncology Center, Hospital Sírio-Libanês, Rua Prof Daher Cutait, 69, São Paulo, SP 01308-060, Brazil; e-mail: fbettoni@mochsl.org.br.

SUPPORT

The São Paulo Research Foundation (FAPESP 2016/05375-0) granted F. Bettoni support for this work.

DATA SHARING STATEMENT

Whole-exome sequencing data from the tumor samples were submitted to the European Genome-Phenome Archive (EGA; www.ebi.ac.uk/ega/) under the accession No. EGAS00001005064.

AUTHOR CONTRIBUTIONS

Conception and design: Marcello M. Queiroz, Rodrigo R. Munhoz, Anamaria A. Camargo, Fabiana Bettoni

Financial support: Anamaria A. Camargo, Fabiana Bettoni

Administrative support: Rodrigo R. Munhoz, Anamaria A. Camargo

Provision of study materials or patients: Rodrigo R. Munhoz, Luiz G.C.A. Lima, Maria Dirlei F.S. Begnami

Collection and assembly of data: Marcello M. Queiroz, Rodrigo R. Munhoz, Larissa M. Souza, Maria Dirlei F.S. Begnami, Fabiana Bettoni

Data analysis and interpretation: Marcello M. Queiroz, Cibele Masotti, Paula F. Asprino, Maria Dirlei F.S. Begnami, Anamaria A. Camargo, Fabiana Bettoni

Manuscript writing: All authors

Final approval of manuscript: All authors

Accountable for all aspects of the work: All authors

AUTHORS' DISCLOSURES OF POTENTIAL CONFLICTS OF INTEREST

The following represents disclosure information provided by authors of this manuscript. All relationships are considered compensated unless otherwise noted. Relationships are self-held unless noted. I = Immediate Family Member, Inst = My Institution. Relationships may not relate to the subject matter of this manuscript. For more information about ASCO's conflict of interest policy, please refer to www.asco.org/rwc or ascopubs.org/po/author-center.

Open Payments is a public database containing information reported by companies about payments made to US-licensed physicians ([Open Payments](http://OpenPayments)).

Rodrigo R. Munhoz

Honoraria: BMS, MSD, Novartis, Sanofi, Merck Serono, Bayer

Consulting or Advisory Role: Sanofi, BMS, MSD, Daiichi Sankyo

Speakers' Bureau: Bristol Myers Squibb, MSD, Novartis, Sanofi

Research Funding: Bristol Myers Squibb, Novartis, MSD, Bayer

Travel, Accommodations, Expenses: Bristol Myers Squibb

No other potential conflicts of interest were reported.

ACKNOWLEDGMENT

We gratefully acknowledge the participation of the patient.

REFERENCES

1. Wang JP, Yao ZG, Sun YW, et al: Clinicopathological characteristics and surgical outcomes of sarcomatoid hepatocellular carcinoma. *World J Gastroenterol* 26:4327-4342, 2020
 2. Hwang S, Lee SG, Lee YJ, et al: Prognostic impact of sarcomatous change of hepatocellular carcinoma in patients undergoing liver resection and liver transplantation. *J Gastrointest Surg* 12:718-724, 2008
 3. Liao SH, Su TH, Jeng YM, et al: Clinical manifestations and outcomes of patients with sarcomatoid hepatocellular carcinoma. *Hepatology* 69:209-221, 2019
 4. Shi D, Sun J, Ma L, et al: Clinical and imaging characteristics of primary hepatic sarcomatoid carcinoma and sarcoma: A comparative study. *BMC Cancer* 20:977, 2020
 5. Yu Y, Zhong Y, Wang J, et al: Sarcomatoid hepatocellular carcinoma (SHC): A case report. *World J Surg Oncol* 15:219, 2017
 6. Zhang C, Feng S, Tu Z, et al: Sarcomatoid hepatocellular carcinoma: From clinical features to cancer genome. *Cancer Med* 10:6227-6238, 2021
-